ISSN 1674-1056
http://cpb.iphy.ac.cn
http://iopscience.iop.org/cpb
中国物理 B
Chinese Physics
中国物理
Chinese Physics B

Magnetism induced by Mn atom doping in SnO monolayer

Ruilin Han(韩瑞林), Yu Yan(闫羽)

Citation: Chin. Phys. B . 2018, 27(11): 117505. **doi:** 10.1088/1674-1056/27/117505
Journal homepage: http://cpb.iphy.ac.cn; http://iopscience.iop.org/cpb

What follows is a list of articles you may be interested in

Progress of novel diluted ferromagnetic semiconductors with decoupled spin and charge doping: Counterparts of Fe-based superconductors

Shengli Guo(郭胜利), Fanlong Ning(宁凡龙)
Chin. Phys. B . 2018, 27(9): 097502. **doi:** 10.1088/1674-1056/27/9/097502

Magnetic properties of AlN monolayer doped with group 1A or 2A nonmagnetic element: First-principles study

Ruilin Han(韩瑞林), Xiaoyang Chen(陈晓阳), Yu Yan(闫羽)
Chin. Phys. B . 2017, 26(9): 097503. **doi:** 10.1088/1674-1056/26/9/097503

Effects of Zr substitution on structural, morphological, and magnetic properties of bismuth iron oxide phases

A Asif, M Hassan, S Riaz, S Naseem, S S Hussain
Chin. Phys. B . 2017, 26(8): 087502. **doi:** 10.1088/1674-1056/26/8/087502

Electronic structures and magnetic properties of Zn- and Cd-doped AlN nanosheets: A first-principles study

Rui-Lin Han(韩瑞林), Shi-Min Jiang(姜世民), Yu Yan(闫羽)
Chin. Phys. B . 2017, 26(2): 027502. **doi:** 10.1088/1674-1056/26/2/027502

Room-temperature ferromagnetism observed in Nd-doped In_2O_3 dilute magnetic semiconducting nanowires

Zhanpeng Lv(吕占朋), Junran Zhang(张军然), Wei Niu(钮伟), Minhao Zhang(张敏昊), Li Song(宋丽), Hairong Zhu(朱海荣), Xuefeng Wang(王学锋)
Chin. Phys. B . 2016, 25(9): 097502. **doi:** 10.1088/1674-1056/25/9/097502

Magnetism induced by Mn atom doping in SnO monolayer

Ruilin Han(韩瑞林)[1,†] and Yu Yan(闫羽)[2]

[1] College of Physics and Electronic Engineering, Shanxi University, Taiyuan 030006, China
[2] Key Laboratory of Physics and Technology for Advanced Batteries (Ministry of Education), Department of Physics, Jilin University, Changchun 130012, China

(Received 21 July 2018; revised manuscript received 5 September 2018; published online 19 October 2018)

The structural, magnetic properties, and mechanism of magnetization of SnO monolayer doped with 3d transition metal Mn atom were studied using first-principles calculations. The calculated results show that the substitution doping is easier to realize under the condition of oxygen enrichment. Numerical results reveal that the spin-splitting defect state of the Mn doped system is produced in the band gap and the magnetic moment of 5.0 μ_B is formed. The induced magnetic moment by Mn_{sub} is mostly derived from the 3d orbital of the doped Mn atom. The magnetic coupling between magnetic moments caused by two Mn atoms in SnO monolayer is a long-range ferromagnetic, which is due to the hole-mediated p–p and p–d interactions. The calculated results suggest that room-temperature ferromagnetism in a SnO monolayer can be induced after substitutional doping of a Mn atom.

Keywords: SnO monolayer, ferromagnetism, first-principles, doping

PACS: 75.50.Gg, 75.50.Pp, 75.75.Lf **DOI:** 10.1088/1674-1056/27/11/117505

1. Introduction

With the discovery and characterization of graphene,[1,2] researchers have increasingly studied the graphene-like two-dimensional (2D) nanomaterials, both theoretically and experimentally. It has been proven that these 2D nanomaterials have novel properties compared with their bulk structures.[3–12] Among them, a newcomer of the 2D material family, metal oxide, has been studied because of its unique and fascinating properties.[13–19]

More recently, attention has been focused on 2D tin monoxide monolayer, which has a unique layered structure in the [001] crystallographic direction with Sn–O–Sn sequence layered, in which bipolar conductivity is easy to achieve.[20,21] Moreover, SnO possesses attractive characteristics such as indirect band gap, comparatively large electron affinity, high electron mobility, and good optical activity.[22–27] Furthermore, few to many-layer SnO films on sapphire and SiO_2 substrates have been synthesized via the pulsed laser deposition (PLD) technique and they exhibit many fascinating properties.[28,29] In addition, it has been reported that ferromagnetism can be obtained in monolayer SnO with hole density of 2–3 $\times$ 10^{14} cm^{-2}.[30] Meanwhile, the results of the structural, optical, and transmission properties indicate that 2D SnO could become the potential candidate in fabricating room-temperature 2D field effect transistor (FET).[22] These theoretical and experimental studies show that a 2D SnO monolayer can be considered as a potential nanoelectronic material, optoelectronic material, and spintronic device. More particularly, SnO-based dilute magnetic semiconductor material is regarded as one of the most promising candidates for spin electronic devices and magnetic devices. However, a pristine pure SnO monolayer does not have intrinsic magnetic properties as a semiconductor. Generally speaking, to obtain a set of integrated electric and magnetic spintronic devices, both spin and charge of electrons combined closely need to turn the semiconductor material into a magnetic material. Exploring and manipulating the magnetism of the 2D material is a research hotspot because of its application in spin electronic devices.[31–35] For example, it has been confirmed theoretically that B-, N-, and F-adsorbed SnO monolayers have magnetic ground states, and B or N contributes less to the total magnetic moments than F.[31] The room temperature ferromagnetism of Mn-doped SnO nano hexagonal plates and cubes has been observed experimentally.[32] Theoretical calculations indicate that ferromagnetism in monolayer SnO can be obtained by hole-doping.[33] Interestingly, it is theoretically predicted that the hole doping of the 2D (single layer) SnO can induce a paramagnetic to ferromagnetic phase transition in this 2D material, because the hole density is usually above 5×10^{13} cm^{-2}.[34] In addition, Wang *et al.* used first-principles calculations to investigate the electronic and magnetic properties of monolayer SnO doped with 3d transition metals from V to Ni.[35] The magnetism of single Mn atom doped SnO monolayer has been studied and a large number of remarkable scientific breakthroughs have been reported.[35] However, the coupling effect between two Mn atoms doped in a SnO monolayer has not been investigated. Therefore, in this paper, we focus on the most intensively investigated electronic structures, magnetic properties, the mechanism of magnetiza-

†Corresponding author. E-mail: hanruilin0116@sxu.edu.cn

© 2018 Chinese Physical Society and IOP Publishing Ltd

tion of single Mn atom and two Mn atoms implanted into SnO monolayer within the framework of a first-principles study.

2. Computational method and details

The electronic and magnetic properties of two-dimensional tin monoxide were calculated within the framework of density functional theory.[36,37] Our calculation was carried out by the Vienna *ab initio* simulation package[36] with a generalized gradient approximation (GGA) functional of PBE.[38] We used the GGA+U scheme to include the strong correlation effects and the exchange parameter for the 3d states of Mn was 3.0 eV, which was chosen based on Ref. [39] and consistent with the values used in Refs. [35] and [40]–[42]. The cutoff energy for the plane wave basis was set to 520 eV. In the process of the structural relaxations and physical properties calculations, we used a Monkhorst–Pack k-point mesh of 5×5×1 to sample the Brillouin zone. To avoid interactions between adjacent layers, a vacuum layer space of 15 Å along the z direction was added. All atoms in the monolayer were relaxed until the convergence threshold of 10^{-6} eV and each atom had a force less than 0.01 eV/Å. The Grimme DFT-D3 approach was adopted to describe the van der Waals interactions for lattice optimization. The doped SnO monolayer was modeled with a supercell consisting of 4×4 two-dimensional unit cells, which contains 64 atoms in total (Fig. 1).

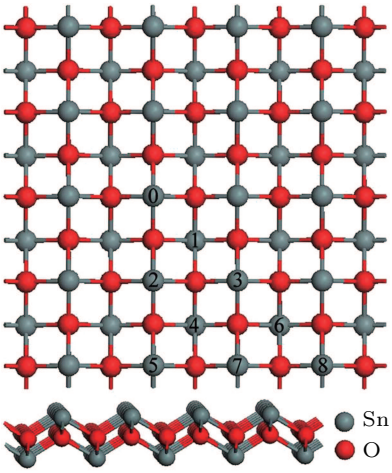


Fig. 1. (color online) Atomic structure of 4×4 monolayer SnO from the top view and the side view. The red and dark grey spheres represent Sn and O atoms, respectively. We take i to mark the doped pair, Mn (0, i), in which the first doped atom occupies the fixed Sn position, labeled 0 in the diagram, and the second doped atom takes position i = 1–8.

3. Results and discussion

Bulk SnO has a tetragonal litharge structure and space group $P4/nmm$, see the ball-and-stick model in Fig. 2(a), and the lattice parameters $a = 3.799$ Å and $c = 4.841$ Å.[43] Our optimized unit-cell bulk and monolayer SnO have lattice constants of $a = b = 3.803$ Å and $c = 4.963$ Å, which agree well with previous findings.[44,45] In Figs. 2(b) and 2(c), the Brillouin zone and band structure of bulk SnO along high-symmetry directions are given. The calculated results show that the bulk SnO is an indirect band gap semiconductor. The valence band maximum (VBM) is located on the Γ–M line, while the conduction band minimum (CBM) is located at the M point, which is in good agreement with previous theoretical results.[31,46–48] SnO has an indirect band gap of 0.37 eV, which is close to the previous findings.[31,46] In its monolayer counterpart, the band gap increases dramatically to 2.96 eV, see Fig. 3(a), which shows that pristine monolayer SnO is a wide band gap semiconductor. The huge change of the band gap will lead to additional potential applications. Moreover, the partial density of states (PDOS) shown in Fig. 3(b) for pristine SnO indicates strong hybridization between the Sn and O states, especially at the edge of the valence band and the conduction band, in agreement with Ref. [35]. In addition, from the calculation results of the pure SnO monolayer, as shown in Fig. 3(b), it can be seen that there is no spin polarization in either the majority-spin channel or minority-spin channel, indicating that the pure SnO monolayer is essentially nonmagnetic. These results show the reliability of our computational methods.

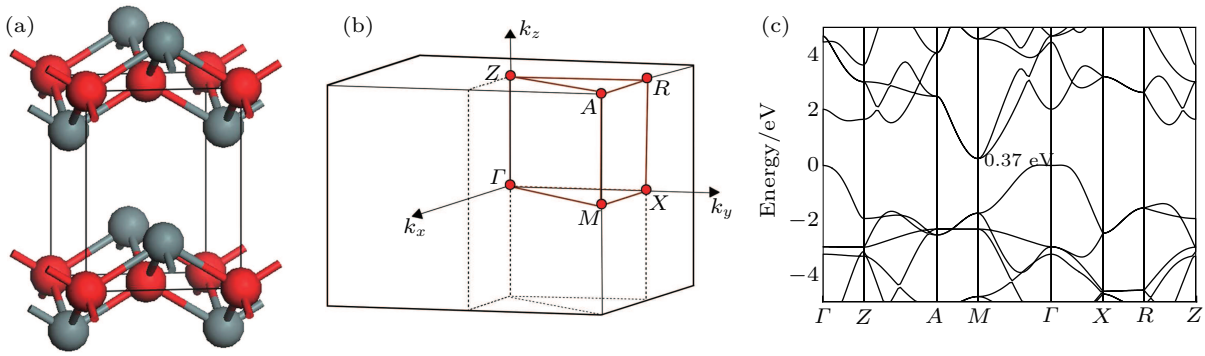


Fig. 2. (color online) (a) Bulk SnO crystal structure, (b) Brillouin zone of SnO. (c) Band structure of SnO along high-symmetry directions.

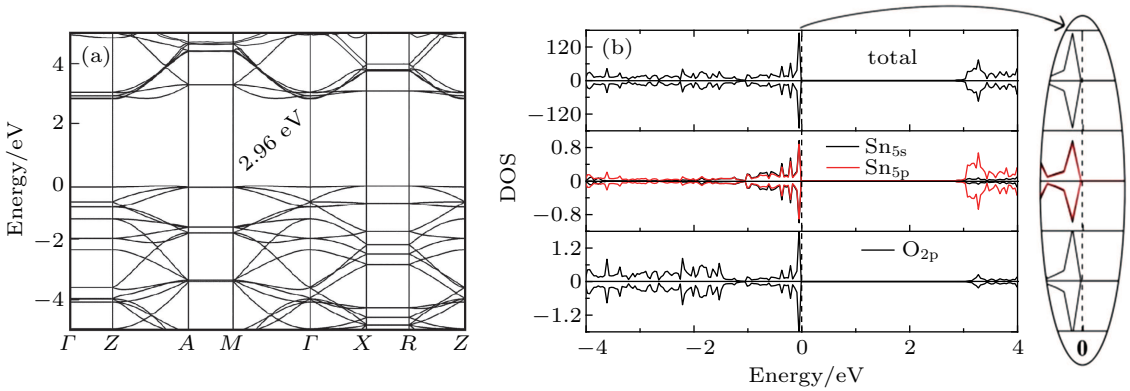


Fig. 3. (color online) (a) Band structure of pure 2D SnO monolayer. (b) Total DOS and partial DOS of p and s states for the Sn atoms and O atom. The Fermi energy is indicated by the dotted line.

We then began to investigate single Mn doped monolayer SnO system ($Sn_{31}MnO_{32}$), in which one Sn atom in the monolayer is displaced by one Mn atom, marked as 0 (impurity concentration of 3.125%), as numbered in Fig. 1. To understand the stability of the doped $Sn_{31}MnO_{32}$ system, the formation energy, E_f, of the $Sn_{31}MnO_{32}$ monolayer was analyzed. As presented in Table 1, the calculated results under both O-rich and Sn-rich growth conditions are −3.76 eV and 0.74 eV, respectively. The calculated results show that the substitution doping is easier to realize under oxygen rich conditions. We also calculated the total energy difference between the spin polarized and non-spin polarized states for the $Sn_{31}MnO_{32}$ monolayer; i.e., $\Delta E_{Spin} = E_{sp}–E_{nsp}$. The calculated total energies of ΔE_{Spin} are negative for the $Sn_{31}MnO_{32}$ monolayer, which indicates that the doped system is more inclined to the spin polarized state, and the ground state of the $Sn_{31}MnO_{32}$ monolayer is magnetic. The optimized bond lengths of Mn–O, the local magnetic moment of dopant Mn with its nearby O atoms, and the total magnetic moment of the monolayer are also listed in Table 1. In Table 1, it can be found that the optimized bond length of Mn–O is 2.215 Å, which is smaller than the pristine Sn–O bond length of 2.252 Å. This phenomenon is mainly attributed to the fact that the ionic radius of Mn (0.46 Å) is shorter than that of Sn (0.69 Å). The local magnetic moments of the doped atom, four O atoms nearest to the dopant, and the total magnetic moment of the $Sn_{31}MnO_{32}$ monolayer are also listed in Table 1. As presented in Table 1, the total magnetic moment of the $Sn_{31}MnO_{32}$ monolayer is 5.000 μ_B induced by a Mn atom. The explanation for this phenomenon is as follows. The Mn has seven valence electrons compare to the host Sn (two valence electrons), this leads to the calculated total magnetic moment exactly equal to the number of the produced holes for the $Sn_{31}MnO_{32}$ monolayer. According to our calculations, the doped Mn atom in the monolayer contributes most to the magnetic moment. The nearest neighbor O atoms around the Mn atom also contribute part of the magnetic moment. The residual magnetic moment is provided by the gap region between the doped atom and the nearest atoms. From DOS and partial DOS in Fig. 4 and spin density distribution in Fig. 5, this viewpoint can be well proven.

Table 1. Calculated results of the energy difference between the spin polarized and non-spin polarized states, optimized Mn–O bond lengths, magnetic moment of the doping atom (M_{Mn}), the nearest neighboring O atoms (M_O) around the doping atom, the total magnetic moment of the monolayer (M_{tot}), and the formation energies E_f of Mn doped SnO monolayer in Sn-rich and O-rich conditions.

System	ΔE_{spin}/eV	Mn–O/Å	M_{Mn}/μ_B	M_O/μ_B	M_{tot}/μ_B	E_f/eV	
						Sn-rich	O-rich
$Sn_{31}MnO_{32}$	–30.2	2.215	4.108	0.592	5.000	0.74	–3.76

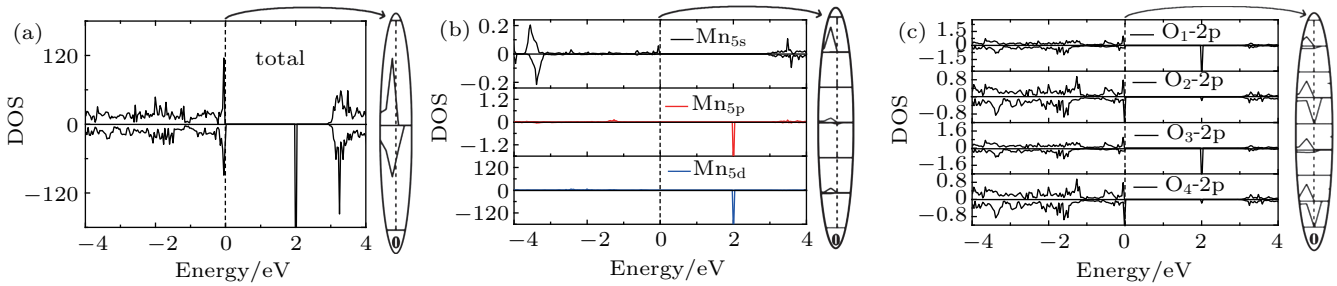


Fig. 4. (color online) (a) The total density of states of $Sn_{31}MnO_{32}$ monolayer, (b) the partial density of states of dopant Mn and (c) its nearest O1-p, O2-p, O3-p, and O4-p states.

Figure 4 presents the total density of states (TDOS) of the $Sn_{31}MnO_{32}$ monolayer, the partial density of states of the dopant Mn, and its nearest four O-2p states. From Fig. 4(a), it can be clearly seen that the distributions of the electronic states for majority-spin and minority-spin orbits are asymmetric. From Figs. 4(b) and 4(c), we can see that the splitting of states near the Fermi energy and in the band gap mainly consists of the 5d states for the dopant, and a part of 2p states for the first neighboring O atoms around the dopant Mn. In other words, the 5d state of the doped Mn atom and the p states of the nearest O atoms around the dopant significantly overlap near the Fermi level and in the band gap, which reveals that the p–d exchange mechanism between the doped Mn atom and four nearby O atoms around the dopant atom in the monolayer can be the origin of the magnetism. Together, the above information illustrates that the $Sn_{31}MnO_{32}$ monolayer exhibits magnetic ground states.

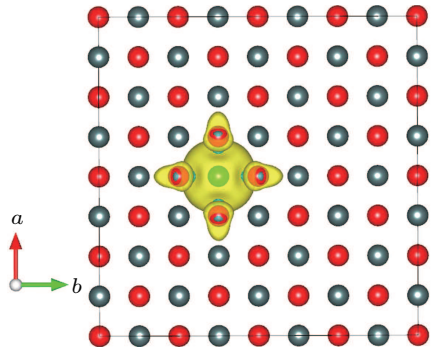


Fig. 5. (color online) The spatial distribution of spin density in the relaxed $Sn_{31}MnO_{32}$. The yellow and blue isosurfaces correspond to the majority and minority-spin densities. The red and dark grey balls represent Sn and O atoms, respectively. The position of the doped atom is marked as green.

Now, we focus on the magnetic coupling between the magnetic moments of two Mn atoms doped SnO monolayer (doping concentration of 6.25%). We substitute two Sn atoms by Mn atoms in SnO monolayer. Eight possible and independent configurations of the two Mn atoms are considered. We take i to mark the doped pair, X (0, i), as shown in Fig. 1, where the first doped atom selects the Sn at a fixed position, marked 0 in Fig. 1, and then the second doped atom labeled by position i = 1–8. We take account of the spin-polarized calculations, ferromagnetic (FM), and antiferromagnetic (AFM) coupling between the moments induced by two dopant atoms in case of each configuration. We calculate the distances between two doped Mn atoms (d_{Mn-Mn}), relative energy ($\Delta\varepsilon$) for the (0, 3) configuration, differences of the FM energy minus the AFM energy ($\Delta E_m = E_{FM} - E_{AFM}$), and total magnetic moment for all the configurations of the doped system. The results are summarized in Table 2, which show that ΔE_m of all configurations is negative, implying that all ground states of $Sn_3Mn_2O_{32}$ are FM. More importantly, we find out that the ΔE_m of all the eight configurations with different distances between two Mn doped atoms are negative from Table 2. The ΔE_m of (0, 8) configuration for the Mn doped SnO monolayer is a small negative value, which still suggests that ferromagnetism may be obtained by doping group Mn atoms in the SnO monolayer. Furthermore, the magnetic moments generated in FM or AFM states of monolayer SnO doped with two Mn atoms are basically consistent with the magnetic moments of $Sn_{31}MnO_{32}$ monolayer. In addition, using mean-field theory, the Curie temperature can be estimated from the energy difference between the system in FM and in AFM states using the equation $\frac{3}{2}k_B T_C = -\Delta E_m/n$, where k_B is the Boltzmann constant and n is the number of the dopants in the system. Our estimated results of eight configurations are 356.3 K, 341.8 K, 338.1 K, 327.3 K, 316.0 K, 304.8 K, 294.8 K, and 272.3 K, respectively. Consequently, our results could provide a theoretical basis for further experimental studies in the future.

Table 2. Calculated distance d_{Mn-Mn} between two dopants; the relative energy, $\Delta\varepsilon$, with respect to that of the (0, 3) structure; the energy difference (ΔE_m) between FM and AFM states, $\Delta E_m = E_{FM} - E_{AFM}$; and the total magnetic moment (M_{tot}) in FM state for doped system $Sn_3Mn_2O_{32}$.

Configuration	d_{Mn-Mn}/Å	$\Delta\varepsilon$/meV	ΔE_m/meV	M_{tot}/μ_B
(0,1)	3.520	130.1	–92.1	9.9982
(0,2)	3.805	109.8	–88.3	9.9987
(0,3)	5.381	0	–87.4	9.9985
(0,4)	6.430	66.3	–84.6	9.9986
(0,5)	7.610	50.7	–81.7	9.9989
(0,6)	8.385	76.8	–78.8	9.9985
(0,7)	8.508	84.8	–76.2	9.9988
(0,8)	10.762	101.4	–70.4	9.9979

Combined with the DOS diagram of SnO monolayer doped with single Mn atom and the spin density spatial distribution diagram of the SnO monolayer doped with two Mn atoms, we can explain the intrinsic reason of the long range ferromagnetic coupling between the magnetic moments induced by the two doped atoms. From Fig. 4, we can find that the density of states of d orbital of doped Mn atom is obviously overlapped with the density of states of p orbital of nearest O atom in the vicinity of Fermi energy level and in the band gap. This indicates the occurrence of p–d hybridization interaction between the Mn dopant and its adjacent O atoms.[49] In addition, figure 4 also shows that the nearest O1-p, O2-p, O3-p, and O4-p states around the doped Mn atom overlap more obviously than other states. This indicates that p–p hybridization interaction occurs between the p state of O atoms around the doped Mn atom. Under such strong p–p and p–d hybridization interactions, there is a coupling between the holes caused by the p-state of the nearest neighbor O atoms around the doped Mn atoms.[49,50] Indeed, the spin density calculated in Fig. 6

indicates that the O atoms between the two doped atoms are polarized to an extent which depends on their direction and distance relative to the Mn site. Furthermore, under the p–d interaction, the spins of O atoms and the dopant have the same polarization direction, which is good for the long-range FM coupling between the two doped atoms.

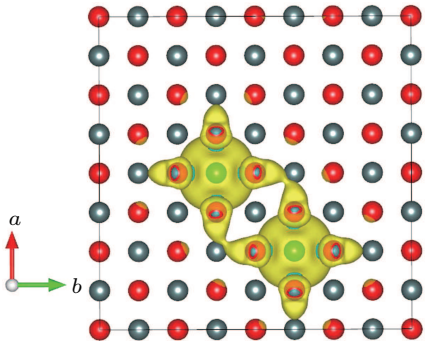


Fig. 6. (color online) The spatial distribution of spin density in the relaxed $Sn_3Mn_2O_{36}$. The yellow and blue isosurfaces correspond to the majority and minority-spin densities. The red and dark grey balls represent Al and N atoms, respectively. The position of the doped atom is marked as green.

4. Conclusion

We used the first-principles methodology to investigate the electronic, structural, and magnetic properties of Mn element doped SnO monolayers with 3.125% and 6.25% Mn concentrations. Our calculation results indicate that the doping actively favors O-rich conditions in comparison with Sn-rich conditions. Our numerical results reveal that a Mn doped SnO monolayer can induce magnetic properties and its magnetic moment is 5.0 μ_B per supercell. The total magnetic moment of the doped SnO monolayer is mainly derived from the dopant Mn atom and four nearest neighboring O atoms. The total magnetic moment of the system is consistent with the number of holes caused by the dopant atom. Furthermore, when we compared our results with those in Ref. [35], we found that magnetic coupling between the magnetic moments introduced by the dual Mn atoms is FM. The p–p and p–d hybridization interactions are responsible for the long-range FM coupling. We believe these results will be useful to further study the properties and applications of the SnO monolayer.

References

[1] Novoselov K, Geim A, Morozo S, Jiang D, Zhang Y, Dubonos S, Grigorieva I and Firsov A 2004 *Science* **306** 666
[2] Novoselov K, Geim A, Morozov S, Jiang D, Katsnelson M, Grigorieva I, Dubonos S and Firsov A 2005 *Nature* **438** 197
[3] Hu P, Wang L, Yoon M, Zhang J, Feng W, Wang X, Wen Z, Idrobo J, Miyamoto Y, Geohegan D and Xiao K 2013 *Nano Lett.* **13** 1649
[4] Mak K F, He K, Shan J and Heinz T F 2012 *Nat. Nanotechnol.* **7** 494
[5] Ma Y, Dai Y, Guo M, Niu C, Lu J and Huang B 2011 *Phys. Chem. Chem. Phys.* **13** 15546
[6] Wang Q, Zadeh K, Kis A, Coleman J and Strano M 2012 *Nat. Nanotechnol.* **7** 699
[7] Tongay S, Zhou J, Ataca C, Lo K, Matthews T, Li J, Grossman J and Wu J 2012 *Nano Lett.* **12** 5576
[8] Li X and Yang J 2014 *J. Mater. Chem. C* **2** 7071
[9] Keyshar K, Gong Y, Ye G, Brunetto G, Zhou W, Cole D, Hackenberg K, He Y, Machado L, Kabbani M, Hart A, Li B, Galvao D, George A, Vajtai R, Tiwary C and Ajayan P 2015 *Adv. Mater.* **27** 4640
[10] Zheng H, Zhang J, Yang S, Du X and Yan Y 2015 *Phys. Chem. Chem. Phys.* **17** 16341
[11] Marks T J and Hersam M C 2015 *Nature* **520** 7549
[12] Golberg D, Bando Y, Huang Y, Terao T, Mitome M, Tang C and Zhi C 2010 *ACS Nano* **4** 2979
[13] Osada M and Sasaki T 2009 *J. Mater. Chem.* **19** 2503
[14] Omomo Y, Sasaki T, Wang T, Watanabe and M 2003 *J. Am. Chem. Soc.* **125** 3568
[15] Osada M, Itose M, Ebina Y, Ono K, Ueda S, Kobayashi K and Sasaki T 2008 *Appl. Phys. Lett.* **92** 253110
[16] Kotani Y, Taniuchi T, Osada M, Sasaki T, Kotsugi M, Guo, F Z, Watanabe Y, Kubota M and Ono K 2008 *Appl. Phys. Lett.* **93** 093112
[17] Osada M, Ebina Y, Fukuda K, Ono K, Takada K, Yamaura K, Takayama-Muromachi E and Sasaki T 2006 *Phys. Rev. B* **73** 153301
[18] Ma R and Sasaki T 2010 *Adv. Mater.* **22** 5082
[19] Coleman J N, Lotya M, O'Neill A, Bergin S D, King P J, Khan U, Young K, Gaucher A, De S and Smith R J 2011 *Science* **331** 568
[20] Pannetier J and Denes G 1980 *Acta Crystallogr. B* **36** 2763
[21] Pan X Q and Fu L J 2001 *J. Electroceram.* **7** 35
[22] Saji K J, Tian K, Snure M and Tiwari A 2016 *Adv. Electron. Mater.* **2** 1500453
[23] Quackenbush N F, Allen J P, Scanlon D O, Sallis S, Hewlett J A, Nandur A S, Chen B, Smith K E, Weil, C, Fischer D A, Woicik J C, White B E, Watson G W and Piper L F J 2013 *Chem. Mater.* **25** 3114
[24] Caraveo-Frescas J A, Nayak P K, Al-Jawhari H A, Granato D B, Schwingenschlögl U and Alshareef H N 2013 *ACS Nano* **7** 5160
[25] Liang L Y, Cao H T, Chen X B, Liu Z M, Zhuge F, Luo H, Li J, Lu Y C and Lu W 2012 *Appl. Phys. Lett.* **100** 263502
[26] Chen P C, Chiu Y C, Zheng Z W, Cheng C H and Wu Y H 2016 *Phys. Status Solidi RRL* **10** 919
[27] Ma Z, Wang B, Ou L, Zhang Y, Zhang X and Zhou Z 2016 *Nanotechnology* **27** 415203
[28] Nomura K, Kamiya T and Hosono H 2011 *Adv. Mater.* **23** 3431
[29] Hosono H, Ogo Y, Yanagi H and Kamiya T 2011 *Electrochem. Solid-State Lett.* **14** H13
[30] Seixas L, Rodin A S, Carvalho A and Neto A H C 2016 *Phys. Rev. Lett.* **116** 206803
[31] Tao J G and Guan L X 2017 *Sci. Rep.* **7** 44568
[32] Hassan Farooq M, Hussain Riaz, Zhang L E, Aslam I, Tanveer M, Shah M W and Zubair Iqbal M 2014 *Mater. Lett.* **131** 350
[33] Houssa M, Iordanidou K, Pourtois G, Afanas'ev V V and Stesmans A 2018 *AIP Adv.* **8** 055010
[34] Seixas L, Rodin A S, Carvalho A and Neto A H 2016 *Phys. Rev. Lett.* **116** 206803
[35] Wang Y R, Li S and Yi J B 2018 *J. Phys. Chem. C* **122** 4651
[36] Kresse G and Furthmüller J 1996 *Phys. Rev. B* **54** 11169
[37] Kresse G and Hafner J 1994 *Phys. Rev. B* **49** 14251
[38] Perdew J P, J Burke K, Ernzerhof M 1996 *Phys. Rev. Lett.* **77** 3865
[39] Zhou F, Cococcioni M, Marianetti C A, Morgan D and Ceder G 2004 *Phys. Rev. B* **70** 235121
[40] Cococcioni M and de Gironcoli S 2005 *Phys. Rev. B* **71** 035105
[41] Wang L, Maxisch T and Ceder G 2006 *Phys. Rev. B* **73** 195107
[42] Jain A, Hautier G, Ong S P, Moore C J, Fischer C C, Persson K A and Ceder G 2011 *Phys. Rev. B* **84** 045115
[43] Izumi F 1981 *Solid State Chem.* **38** 381
[44] Seixas L, Rodin A S, Carvalho A and Neto A H C 2016 *Phys. Rev. Lett.* **116** 206803
[45] Izumi F 1981 *J. Solid State Chem.* **38** 381
[46] Varley J B, Schleife A, Janotti A and Van de Walle C G 2013 *Appl. Phys. Lett.* **103** 082118
[47] Zhou W and Umezawa N 2015 *Phys. Chem. Chem. Phys.* **17** 17816
[48] Granato D B, Albar A and Schwingenschlogl U 2014 *Europhys. Lett.* **106** 16001
[49] Shen L, Wu R Q, Pan H, Peng G W, Yang M, Sha Z D and Feng Y P 2008 *Phys. Rev. B* **78** 073306
[50] Long R N 2009 *Phys. Rev. B* **80** 115212